FATIGUE CRACK PROPAGATION IN AEROSPACE ALUMINUM ALLOYS

R.P. Gangloff[1], R.S. Piascik[2], D.L. Dicus[3] and J.C. Newman, Jr.[4]

Abstract

This paper reviews fracture mechanics based, damage tolerant characterizations and predictions of fatigue crack growth in aerospace aluminum alloys. The results of laboratory experimentation and modeling are summarized in the areas of: (a) fatigue crack closure, (b) the wide range crack growth rate response of conventional aluminum alloys, (c) the fatigue behavior of advanced monolithic aluminum alloys and metal matrix composites, (d) the short crack problem, (e) environmental fatigue and (f) variable amplitude loading. Remaining uncertainties and necessary research are identified. This work provides a foundation for the development of fatigue resistant alloys and composites, next generation life prediction codes for new structural designs and extreme environments, and to counter the problem of aging components.

I. Introduction

The fracture mechanics approach to fatigue crack propagation quantitatively couples laboratory studies on alloy performance and fatigue mechanisms with damage tolerant life prediction methods through the concept of growth rate similitude. This method, illustrated in Figure 1, is traceable to the seminal results of Paris and coworkers for the case of moist air environments[1] and is outlined in current textbooks[2]. Subcritical fatigue crack propagation is measured in precracked laboratory specimens according to standardized methods[3]. Crack length (a) versus load cycles (N) data are analyzed to yield a material property; averaged fatigue crack growth rate (da/dN) as a function of the applied stress intensity range, ΔK. ΔK is the difference between maximum (K_{max}) and minimum (K_{min}) stress intensity values during a load cycle. Paris experimentally demonstrated the principle of similitude; that is, equal fatigue crack growth rates are produced for equal applied stress intensity ranges, independent of load, crack size and component or specimen geometry[1]. Wei and coworkers extended this concept to describe corrosion fatigue crack propagation in aggressive gas and liquid environments[4].

The similitude principle enables an integration of laboratory da/dN-ΔK data to predict component fatigue

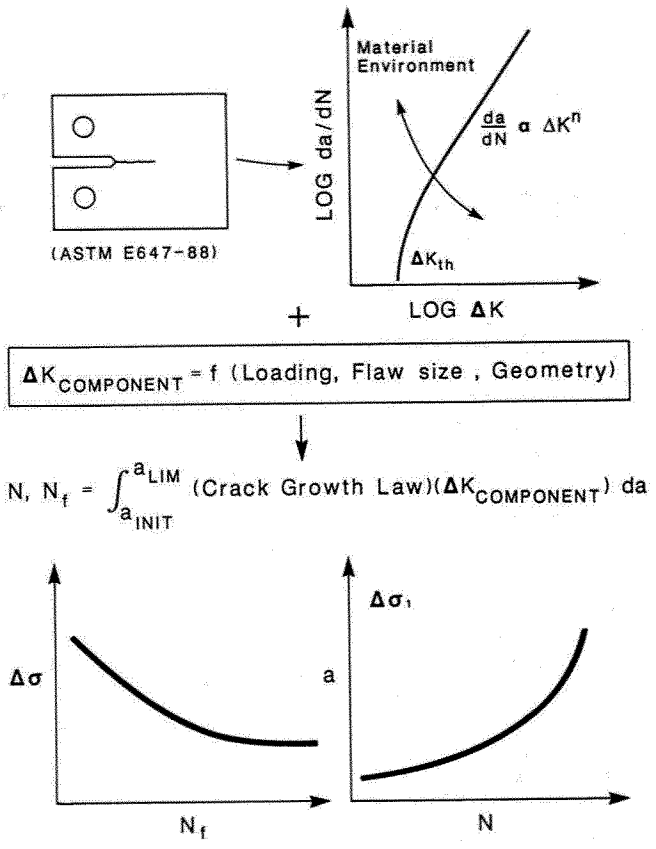

Figure 1. *Fracture mechanics approach to fatigue crack growth: material characterization and component life prediction.*

behavior, in terms of either applied stress range ($\Delta\sigma$) versus total life (N_f) or crack length (a) versus load cycles (N), for any initial defect size and component configuration. These calculations require component loading and stress analyses, initial crack size and shape, and a component stress intensity solution. This method has been developed for complex structural applications in the energy, petrochemical and

[1] Department of Materials Science, School of Engineering and Applied Science, University of Virginia, Charlottesville, VA, 22901.

[2] Formerly, Graduate Student, Department of Materials Science, University of Virginia; Currently, Mechanics of Materials Branch, Materials Division, NASA Langley Research Center, Hampton, VA, 23665.

[3] Metallic Materials Branch, Materials Division, NASA Langley Research Center, Hampton, VA, 23665.

[4] Mechanics of Materials Branch, Materials Division, NASA Langley Research Center, Hampton, VA, 23665.

transportation sectors[5-9]. In these cases classical fatigue design rules, based on smooth specimen data and which do not generally account for time dependent environmental effects, are being challenged by damage tolerant crack growth procedures.

Damage tolerant design requirements for aerospace structures stimulated the development of fatigue crack growth life prediction methodologies based on fracture mechanics. In 1979 two round robin programs were initiated in the United States[10] and Europe[11] to implement the approach illustrated in Figure 1 for aerospace components and mission loading spectra. The methods and models used in these programs can be categorized into either empirical (viz., yield zone or crack closure) or analytical crack closure models. Each was based on modeling plasticity effects and most accounted for load-interaction effects such as crack growth retardation and acceleration and mission-relevant load spectra.

Empirical yield zone models were generally based on the Willenborg et al. model[12], but modified to improve its accuracy[13,14]. The yield zone models require several constants, other than the standard constant amplitude crack growth properties, to accurately predict crack growth under aircraft loading. Empirical crack closure models also require several empirical constants to account for variations in crack opening stresses during spectrum loading[15,16]. Analytical crack closure models predict the variation in crack opening stresses during a load history[17]. These methods and models have been incorporated into fatigue damage tolerance computer codes for aerospace structures, including CRKGRO[18], NASA FLAGRO[19], NASCRAC[20] and FASTRAN[21].

The results from these studies indicate that the advanced yield zone and crack closure based models reasonably predict crack growth lives under aircraft spectrum loading, provided that the models are adjusted based on results from similar materials and loading[10,11]. The studies also demonstrate that the inclusion of both crack growth retardation and acceleration is necessary to give accurate life results. The significance of crack closure, as defined in an ensuing section, in explaining and modeling fatigue crack growth is illustrated in both studies. Further work is deemed to be necessary to develop truly predictive methods for fatigue crack growth life prediction.

II. Objective

The objective of this paper is to review the state-of-the-art regarding fracture mechanics based damage tolerant characterizations and predictions of fatigue life in aerospace aluminum alloys. Emphasis is placed on recent laboratory experiments and models used in life prediction codes. The following sections summarize research over the past 15 years on: (a) fatigue crack closure, (b) the wide range da/dN-ΔK response of aluminum alloys, (c) the fatigue behavior of new monolithic aluminum alloys and metal matrix composites, (d) the short crack problem, (e) environmental fatigue and (f) variable amplitude loading. The results of this work are being incorporated into next generation fatigue damage tolerant life prediction codes for new structural designs, intended for extreme environments, and to counter the problem of aging components.

III. Fatigue Crack Closure

A notable development from fatigue crack propagation research has been the concept of crack closure[22]. While stress intensity similitude was initially based on applied ΔK, as indicated in Figure 1, experiments and modeling demonstrate that crack surfaces can contact during the unloading portion of the fatigue cycle at positive applied stress levels. Such contact shields the crack tip from further unloading; the cyclic strain range at the crack tip is accordingly reduced from that level typical of the complete excursion of stress intensity from K_{min} to K_{max}. Crack closure causes reductions in growth rates compared to the values typical of unhindered crack opening at the same applied ΔK range[23-28]. Extrinsic crack growth is that which is closure-influenced, while fatigue under closure-free loading is said to be intrinsic.

An effective stress intensity range (ΔK_{eff}), defined as $K_{max} - K_{opening}$, reasonably correlates da/dN in a form similar to that indicated for applied ΔK; Figure 1. The extent of crack closure, that is the magnitude of ΔK_{eff}, depends on applied ΔK, stress ratio ($R = K_{min}/K_{max}$), stress level, crack length, specimen thickness, alloy microstructure and environment. Closure provides an explanation for the effects of a variety of metallurgical, mechanical and environment chemistry variables.

All known mechanisms for premature crack surface contact or closure act in the wake of the propagating fatigue crack[27]. Three specific shielding mechanisms are illustrated in Figure 2. Plasticity induced closure, Figure 2a, arises from an interference between mating crack surfaces which were

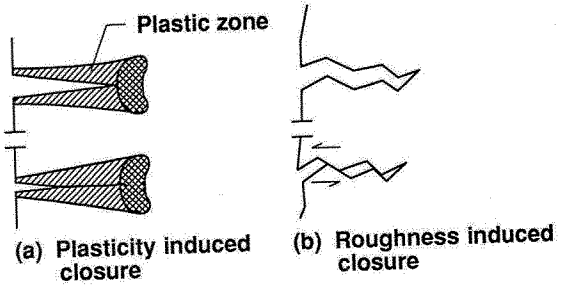

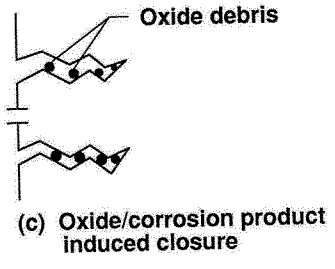

Figure 2. *Mechanisms for crack closure: (a) plasticity induced closure, (b) roughness induced closure and (c) corrosion debris induced closure (After Ritchie[27]).*

permanently deformed as the crack tip passed through the plastic zone. Plasticity induced closure is by far the most dominant form of closure and was the first to be extensively studied in experiments and numerical analyses. This closure mechanism is thought to be dominant under plane stress deformation, typical of higher ΔK levels. At very high ΔK, where elastic constraint is no longer operative and the material is fully plastic, plasticity induced closure becomes insignificant. Little is known about the effect of plasticity induced closure on near-threshold fatigue crack propagation. Other forms of closure, such as roughness or oxide/corrosion product induced closure occur, but they have yet to be quantified. Roughness induced closure, shown in Figure 2b, arises from premature contact of crack surface asperities which may be pronounced for specific microstructure, deformation mode and environment conditions. Roughness induced closure is significant at near-threshold stress intensities, where crack tip opening displacements are comparable to fracture surface asperity heights, and when Mode II displacements exist. As a third mechanism for closure, fatigue crack growth rates are reduced when crack surface corrosion products reach a thickness comparable to crack opening displacements, Figure 2c. Here, the crack is wedged open at stress intensities above K_{min}, resulting in reduced crack tip damage. Measurements of closure, or more correctly the opening load, from compliance methods provide a means of approximately calculating ΔK_{eff}, but are not able to distinguish between the various forms of closure.

The crack closure concept has been extensively used to correlate crack growth rate data under constant amplitude loading. In principle such results provide intrinsic material property data for component fatigue life prediction. An example for crack growth rate data on aluminum alloy 2024-T3 center crack tension panels is shown in Figure 3. Symbols (x) indicate experimental results obtained from 2.3 mm thick specimens loaded over a wide range of stress ratios ($-2 \leq R \leq 0.7$) and applied stress levels ($10 \leq S_{max} \leq 280$ MPa)[29-31]. Rather than being based on compliance measurements, the plastic zone corrected effective stress intensity factor range (ΔK_{eff}) was calculated from crack opening stress equations developed from a plasticity induced closure model[17]. This model requires a "constraint" factor (α) which approximates the effect of triaxial constraint on yielding ahead of the crack tip. For plane stress, α equals 1.0 and for plane strain α is 3.0. For the thin material, a constraint factor of 1.3 was selected for rates greater than 7.5×10^{-7} m/cycle (end of the transition from flat to slant crack growth) and $\alpha = 1.73$ for rates less than 9×10^{-8} m/cycle (beginning of the transition from flat to slant crack growth). For intermediate rates, α was assumed to vary linearly from 1.3 to 1.73 and with the logarithm of da/dN. Crack growth on a 45° plane through the thickness is indicative of plane stress conditions, while flat crack growth indicates nearly plane strain constraint. These particular values of α were selected to correlate crack growth rate data for the various stress ratio conditions. The open symbols at extremely high rates are obtained from monotonic fracture tests on 1.8 mm thick specimens. Stable crack extension was treated as crack growth in a single cycle. (These results show that stable crack extension during monotonic loading can be treated as a continuation of the fatigue crack growth rate curve[32].)

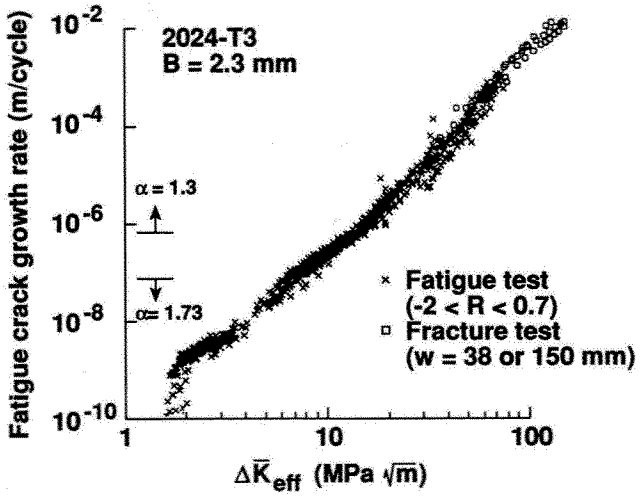

Figure 3. *Plastic zone corrected effective stress intensity factor correlations for wide range in R and stress levels for an aluminum alloy.*

For aluminum alloys, measurements and calculations from plasticity induced closure models show that, even in the near-threshold regime, closure can amount to a large percentage of the applied maximum load[17]. Figure 4 shows measured (solid symbols)[31] and calculated (open symbols) threshold stress intensity range (ΔK_{th}) values for 2024-T3 sheet material as a function of stress ratio. (ΔK values for negative stress ratios are K_{max} values.) The analysis assumed that the effective threshold was 1.65 MPa√m. A 6% load shedding method was used in the tests, while two analysis methods were used, including an incremental smooth and the 6% method[3]. These results show that the rise in the threshold value can be

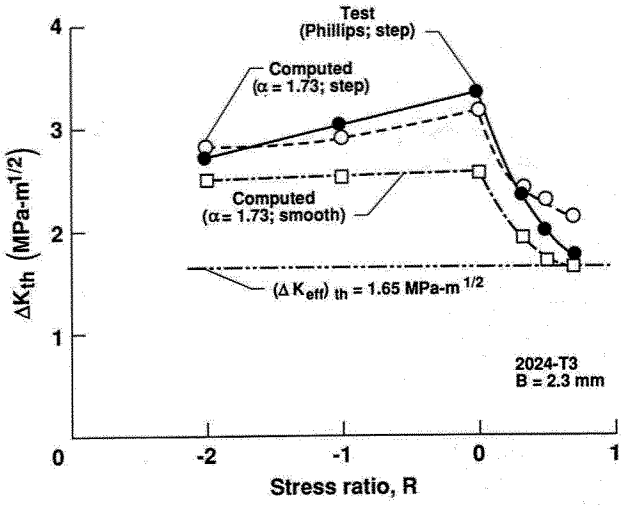

Figure 4. *Comparison of experimental and computed fatigue crack growth thresholds for an aluminum alloy as a function of stress ratio.*

calculated from a plasticity induced closure model. Some discrepancies were observed between experiments and analyses for the high R ratio conditions, however, the test results were bounded by the two load shedding procedures.

The plasticity induced closure model has also been used to analyze roughness or corrosion debris induced closure and to demonstrate the effectiveness of these shielding mechanisms. Figure 5 shows how the inclusion of an interference particle onto the crack surface affects the crack opening stress, S_{op}.

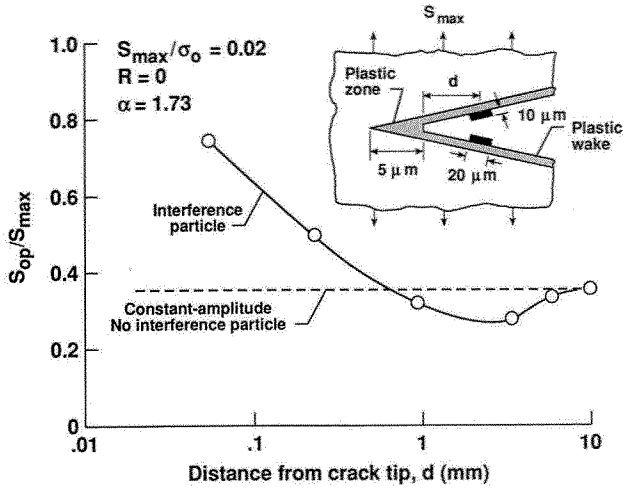

Figure 5. *Influence of an interference particle on crack opening stresses under constant amplitude loading for an aluminum alloy.*

The particle was arbitrarily chosen as a two dimensional rectangle (10 μm by 20 μm by thickness) located at a distance, d, from the crack tip. The dashed line shows the steady-state results under constant amplitude loading (S_{max} to flow stress, σ_o, ratio of 0.02) and with a constraint factor of 1.73 (Irwin plane strain condition). A particle located 10 mm from the crack tip had no effect on crack opening stress. As the particle was placed closer to the crack tip, however, complex closure behavior was revealed. After an initial drop in the opening stress for a particle placed between 10 and 1 mm of the crack tip, a steady rise in S_{op} was observed for d less than 1 mm. These results suggest that the interference must be extremely close to the crack tip to influence crack opening stresses and to enhance crack tip shielding. These results also show that plasticity induced closure from continuum mechanics is active at extremely small plastic zone sizes (about 5 μm). This behavior is due to the fact that crack opening stresses are controlled by the relative ratio of the plastic zone size to crack surface opening displacement, and not by the absolute size of the plastic zone.

IV. Fatigue Crack Propagation Data Bases: Aluminum Alloys

Conventional Aluminum Alloys

The general fatigue crack propagation (FCP) behavior of structural aluminum alloys stressed in vacuum is approximated by an empirical relationship developed by Speidel[33]:

$$da/dN = 1.7 \times 10^{6} (\Delta K/E)^{3.5}$$

$$\Delta K_{th} = 2.7 \times 10^{-5} E$$

where da/dN is in units of m/cycle, ΔK and ΔK_{th} are in MPa$\sqrt{m}$ and the modulus of elasticity (E) is in MPa. This result should be employed as a guideline only, and does not describe the behavior of novel alloy microstructures, crack closure dominant situations, short crack effects and the influence of environment. Crack wake closure and environment may particularly alter near-threshold and the power-law (Paris) regimes of da/dN-ΔK behavior.

Considerable research has been directed towards understanding the fatigue crack growth properties of conventional high strength aluminum alloys; particularly, ingot metallurgy (I/M) 2XXX (Al-Cu) and 7XXX (Al-Zn-Cu-Mg) alloys. The rate of fatigue crack growth has been studied over a wide range of ΔK and R in alloys 2024 and 7075, Figures 6 and 7, respectively[29-31,34]. As R increases from -1.0 to 0.70

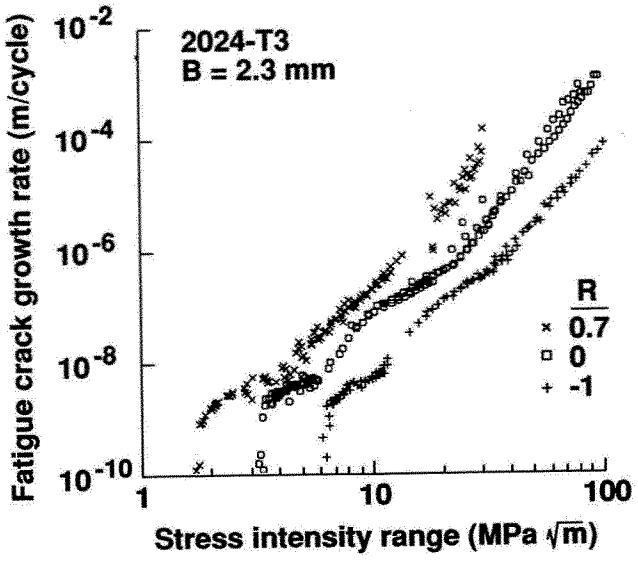

Figure 6. *Fatigue crack growth in alloy 2024 for a wide range of ΔK, at R = -1, 0 and 0.7.*

for alloy 2024 (Figure 6) and from 0 to 0.88 for alloy 7075 (Figure 7), near-threshold and Paris regime fatigue crack growth rates increase by five to fifteen-fold. This large mean stress effect is the result of decreased plasticity, roughness and oxide induced crack closure[22]. Specifically, high R limits crack wake surface contact during unloading, and results in increased crack tip driving force and higher da/dN when plotted versus applied ΔK.

Extensive research has been performed on fatigue threshold stress intensity concepts. While specific data are abundant, little is known about crack tip damage mechanisms and particularly environmental effects[35,36]. Figure 8 shows that laboratory air is damaging to 2000 and 7000 series alloys[34,37-43]. Near-threshold, intrinsic fatigue crack growth rates are a factor of 10 to 100 higher compared to vacuum results. The data shown in Figure 8 also reveal that 7000 series alloys exhibit increased fatigue crack growth rates compared to 2000 series alloys, suggesting an increased environmental sensitivity for 7000 materials.

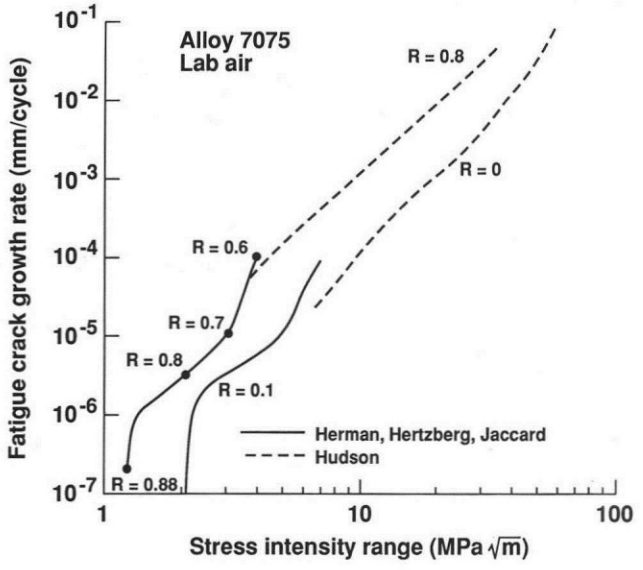

Figure 7. *Fatigue crack growth in alloy 7075 for a wide range of cyclic stress intensities, for R ranging from 0 to 0.88.*

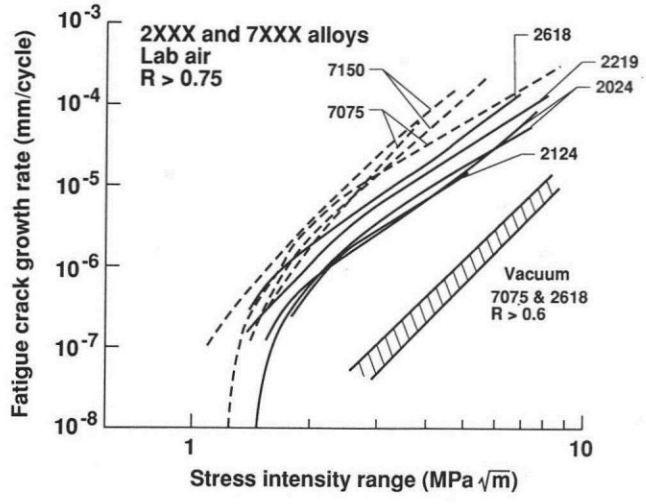

Figure 8. *A comparison of intrinsic (high R) fatigue crack growth rates in 2XXX and 7XXX series aluminum alloys for moist laboratory air and vacuum.*

Microstructural Effects

Systematic studies of conventional high strength aluminum alloys established how different components of the microstructure contribute to fatigue crack propagation. As a general principle, irreversible cyclic plastic strain results in crack tip damage and is recognized as the controlling parameter during fatigue crack propagation. Microstructural features which promote a heterogeneous distribution of concentrated plastic strain lead to undesirable local stress concentration and enhanced crack growth rate[44]. Additionally, however, microstructural effects on FCP are traceable to crack closure[45] and environmental mechanisms[46]. Identification of the precise factor which influences cracking is often ambiguous.

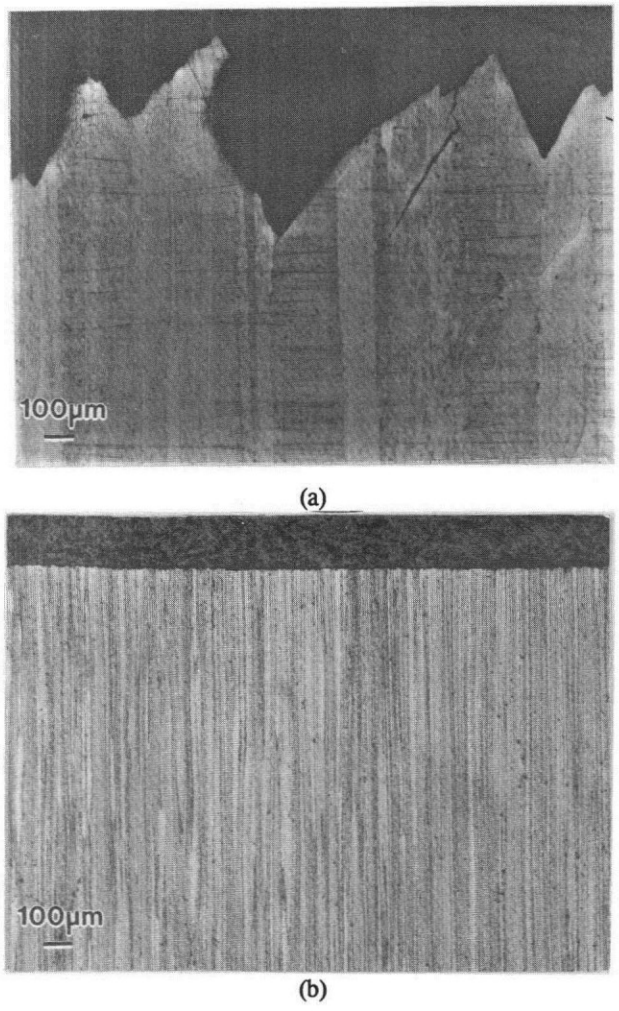

Figure 9. *Micrographs of: (a) the tortuous fatigue crack path in an I/M Al-Li alloy (2090), and (b) the flat fatigue crack path in an Al-8Fe-1.4V-1.7Si P/M alloy (after Bray[51]).*

Aluminum alloys are strengthened by complex precipitate microstructures which inhibit dislocation motion. These microstructures consist of fine metastable hardening (precipitate) particles, high temperature dispersoids for grain size control and coarse impurity-based intermetallic (constituent) particles . Such second phases influence fatigue response in ways that strongly depend on loading conditions and environment[26,44-46]. Metastable strengthening precipitates

(eg., S', θ' or δ') have the strongest influence on FCP. The volume fraction, size, coherency and distribution of such shearable precipitates and precipitate free zones associated with grain boundary particles control deleterious plastic strain localization at all levels of ΔK. Shearable matrix precipitates control the degree of slip planarity within the crack tip cyclic plastic zone. Microscopic cracking occurs along regions of intense slip ahead of the crack tip; Figure 9a shows a typical slip band fatigue fracture morphology for an Al-Li alloy. The influence of this microstructural feature is complex. It is likely that da/dN is intrinsically increased by cracking along localized slip bands[44] and by planar slip enhanced hydrogen embrittlement[46]. Planar slip also promotes crack surface roughness; closure based reductions in da/dN may also be realized[26,45].

Advanced Alloys

Many advanced high strength aluminum alloys have been developed in recent years with the aim of increased stiffness, decreased density and improved elevated temperature resistance. Promising materials include ingot metallurgy (I/M) Al-Li-based alloys, powder metallurgy (P/M) alloys and metal matrix composites (MMC). Lithium addition increases the elastic modulus and decreases the density of precipitation strengthened alloys. Alloys of commercial interest include Al-Li-Cu-Zr (2090 and 2091), Al-Li-Cu-Mg-Zr (8090 and 8091) and weldable Al-Li-Cu-Mg-Ag-Zr (Weldalite). High strength is achieved in powder metallurgy aluminum alloys by rapid solidification and consolidation which result in dispersions of fine intermetallic compounds, dramatically refined grain size, limited undissolved constituents and fewer inhomogeneities when compared to I/M alloys. Examples include Al-Zn-Mg-Co (7091), high temperature experimental alloys Al-5Ti-5Nb, Al-5Er-9Zr, and Al-Fe-Si-V, and lithium based alloys such as Al-Li-Cu-Mg-Zr (644B). Discontinuous metal matrix composites attain enhanced strength and stiffness by the addition of reinforcing chopped fibers, whiskers or particles to an aluminum alloy matrix. Silicon carbide whisker or particle based composites with a 2XXX or 6XXX matrix are particularly attractive because they exhibit essentially isotropic properties and are shaped using conventional methods.

Laboratory data demonstrate that the various advanced aluminum alloys exhibit significantly different crack growth kinetics, particularly when studied at low mean stress intensity levels. Notably, several of these alloys exhibit improved crack growth rate properties, attributable to enhanced crack closure. Lithium based alloys exhibit substantially lower fatigue crack growth rates compared to conventional alloys and the new powder metallurgy alloys. This behavior is illustrated in Figure 10. In addition to lower da/dN, Li based I/M alloys exhibit higher ΔK_{th} (3 to 4 MPa$\sqrt{m}$) compared to P/M alloys (1 to 2.2 MPa$\sqrt{m}$) and discontinuous MMCs (2 to 3 MPa$\sqrt{m}$)[47-51]. Al-Li alloys are strengthened by shearable precipitates and exhibit a tortuous crack path morphology, Figure 9a, resulting in large crack tip shielding effects[45]. At high R, the dashed line in Figure 10, Li based I/M alloys have reduced closure, resulting in increased fatigue crack growth rates and lower thresholds. These FCG rates are comparable to the values for the P/M and discontinuous MMC alloys. P/M and discontinuous MMC fatigue cracking is characterized by low closure, resulting from flat and featureless crack paths, Figure 9b[51]. Crack growth rates are accordingly increased and ΔK_{th} values are decreased.

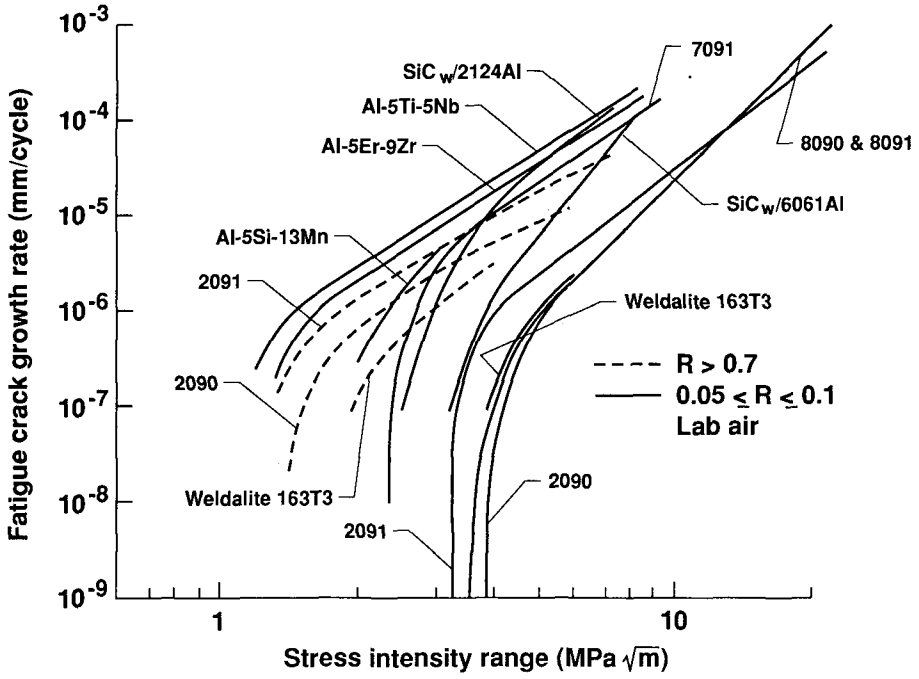

Figure 10. *Comparison of the fatigue crack growth characteristics of high strength I/M Al-Li alloys, P/M aluminum alloys and discontinuously reinforced aluminum alloy MMCs.*

V. Short Crack Problem

During the last decade, the growth behavior of small or short fatigue cracks[5], sized between 5 μm and 5 mm, in metallic materials has received world-wide attention[52-59]. When correlated based on linear elastic fracture mechanics and applied ΔK, short cracks can grow at abnormally rapid rates and well below the large crack threshold for $R > 0$ loading in aluminum, aluminum-lithium, and titanium alloys[53]. For steel, however, short crack and large crack behaviors are nearly identical, except for load histories which include compression[53], or for fatigue in aggressive environments[57,58]. Such observations have caused concern in the aerospace industry. At stress concentrations typical of aircraft structures, short cracks initiate very early in life if the applied stress levels are above the fatigue limit. Because the initiation and short crack growth regimes are a substantial fraction of total life, erroneous and nonconservative predictions of the growth rates of short cracks has major impact on the fracture mechanics approach indicated in Figure 1. As an example, 90% of the life of a notched specimen of 2024-T3 aluminum alloy is associated with the growth of cracks from 20 μm to 2 mm for $R = -1$ loading; this proportion of life falls to about 55% for high R conditions[52]. Similarly, 80% of the total life of a welded steel pipe carrying embrittling H_2S contaminated oil was associated with fatigue crack growth from 0.5 to 21.0 mm, with final failure at a crack length of 10 mm[8].

The growth of short cracks is strongly influenced by load history, stress level, material and environment. The growth differences between short and long cracks, at the same applied ΔK, are more pronounced for load histories which include compressive loading, high stress levels and low R, for alloys which exhibit extreme crack surface roughness, and for aqueous environments. For example, short crack growth behavior in tests with only positive loading is nearly the same as the behavior of large cracks for growth above the large crack threshold[52].

There are four accepted mechanisms for anomalous short crack behavior; each can contribute to fatigue in a given material/environment system[55]. They are: (1) the loss of similitude which occurs when stress levels are too high and small-scale yielding is exceeded, (2) local microstructural features which either promote noncontinuum plastic deformation and thus rapid crack growth, or cause severe retardation, (3) the lack of crack closure in the early stages of crack growth when the shielding wake length is limited, and (4) the unique gas or aqueous electrolyte chemistry which may develop within a short occluded crack. The exact definition of a short crack depends on the mechanism(s) for the rapid growth rates.

Perhaps the most significant feature of short crack growth behavior is propagation at applied ΔK levels below the long crack threshold. This behavior impacts design life calculations. Long crack data that include a threshold clearly cannot be used in analyses that treat the early stages of crack growth in aluminum alloys because such data lead to prediction of infinite life for crack sizes as much as an order-of-magnitude larger than crack sizes that have been observed to grow to failure[52,53]. Thus, the use of long crack thresholds in damage tolerance and durability analyses is likely to be nonconservative. This topic should be thoroughly investigated, particularly for a variety of alloys, microstructures and environments.

Typical results on short crack growth behavior in 2024-T3 aluminum alloy are shown in Figure 11. These data are from single-edge-notch tension specimens tested under $R = -2$ loading[52], with each applied stress level noted by a particular symbol. The solid curves show predictions from the analytical closure model for various maximum applied stress

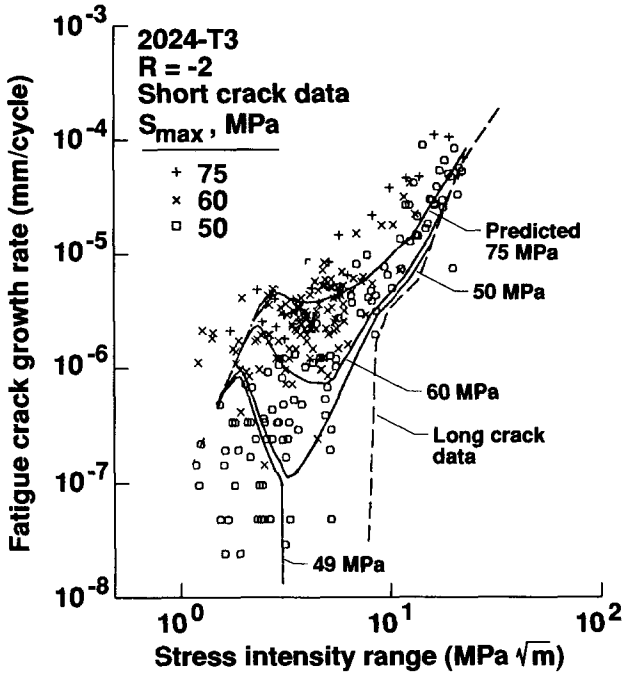

Figure 11. *Comparison of short and long crack growth rate behavior for 2024-T3 aluminum alloy.*

levels[60]. The dashed line shows long crack data generated under the same conditions. These results show a strong influence of stress level (S_{max}) on the growth rates for short cracks, which grow faster at higher stress levels for the same value of applied ΔK. To make predictions, an initial crack size was selected as 3 μm by 12 μm by 0.4 μm and an effective stress intensity factor threshold, $(\Delta K_{eff})_{th}$, was chosen as 1.05 MPa$\sqrt{m}$ to fit fatigue life (S-N) data[52]. Short cracks in aluminum alloys tend to initiate at inclusion particle clusters or at voids on or near the notch root surface. Material defects in test specimens were observed to be about the same size as assumed in the analysis. The predictions from the model show a similar stress level effect on the growth of short cracks. Although the initial crack growth rates from the model were in qualitative agreement with measured rates, the model predicted

[5] The "short" crack is often defined as having a physically limited length, but intersecting many grains along a substantial crack front. The "small" crack is defined as being contained within a single grain; both length and crack front perimeter are of restricted dimension[55]. Short is used in this review for each type of crack.

slower rates in the mid-range than those measured. The predicted rates approach the long crack values more rapidly than in the test. Irwin's plane strain condition was assumed to occur for the growth of short cracks at the notch root. The actual behavior, however, may be closer to plane stress for these cracks.

At an applied stress of 50 MPa, model predictions show that the short crack nearly arrested at a ΔK level of 3 MPa$\sqrt{m}$. A prediction for an applied stress level of 49 MPa demonstrated that a short crack can initiate and grow from a defect, but as the crack opening stresses rise, the crack can be arrested. The data and model predictions presented in Figure 11 strongly suggest that the lack of crack wake closure is a dominant mechanism for the anomalously rapid and subthreshold growth of short cracks in aluminum alloys. As such, it is possible to describe the crack size effect analytically for implementation in life prediction codes.

VI. Environmental Effects

The surrounding environment, perhaps more than any other variable, exacerbates rates of fatigue crack propagation in aluminum alloys compared to vacuum or inert gases[46]. Crack tip damage accumulates with loading due to the synergistic interaction between cyclic plastic deformation and localized chemical reaction. While stress corrosion cracking (SCC) may occur during fatigue loading[61], cyclic deformation promotes environmental fatigue (or corrosion fatigue) below the threshold stress intensity for monotonic load cracking, K_{ISCC}. As SCC-resistant aluminum alloys are developed, sub-K_{ISCC} environmental fatigue assumes paramount importance[62].

The application of fracture mechanics to corrosion fatigue crack propagation has progressed over the past 25 years[4]6. Notable advances include: (a) the demonstration of ΔK similitude[63], (b) developments of experimental methods[64], (c) phenomenological characterizations of crack growth rate behavior, first for high strength, then low strength alloys[46], (d) identification of crack closure, threshold and short crack issues[22,54], (e) scientific studies of fatigue mechanisms[4] and (f) syntheses of life prediction methods[5]. This work shows that variables which are not important to mechanical fatigue critically affect cracking in aggressive gases and liquids[46].

Embrittling Environments

Pure water vapor, moist air, and aqueous electrolytes with halogen ions (eg. Cl^-) enhance fatigue crack propagation in aluminum alloys near ambient temperature. An example is presented in Figure 12 for an advanced Al-Cu-Li alloy (2090)[42,48,66]. A constant ΔK and constant K_{max}-increasing R method produced these data; R increased from 0.1 to 0.9 as ΔK was decreased in discrete steps at K_{max} = 17 MPa$\sqrt{m}$. Similar, slow FCP rates are produced by loading in ultra-high vacuum, purified helium and molecular oxygen. Increased fatigue crack growth rates are recorded for high purity water vapor and aqueous NaCl solution with constant immersion and applied

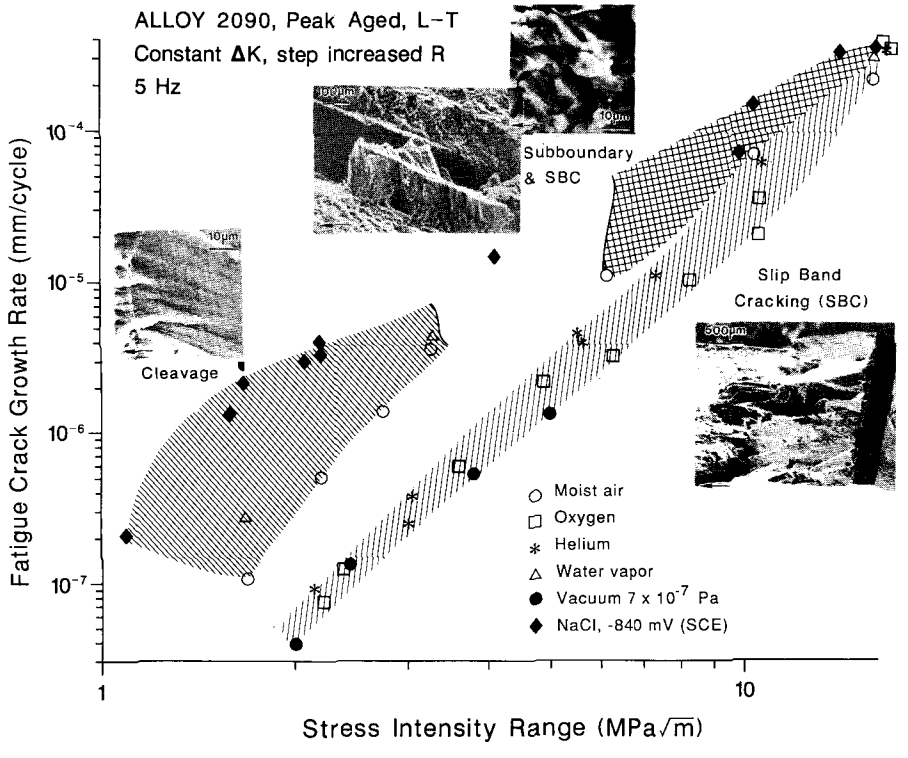

Figure 12. *Environmental effects on fatigue crack growth kinetics and microscopic cracking modes for Al-Li-Cu alloy 2090.*

[6] Environment adversely affects each of the progressive stages of cyclic plastic deformation, microcrack nucleation and crack propagation which constitute fatigue failure of a metal[65].

anodic polarization. Moist air is an aggressive environment relative to vacuum, with water vapor being the likely aggressive specie given the inert character of O_2.

Environmental effects on da/dN are accompanied by transitions in the microscopic fatigue crack path. For inert environments, fatigue proceeds by either {111} type slip band cracking in alloys which exhibit localized planar slip, or by crack tip shear and blunting advance leading to striations. Environmental fatigue progresses along either high angle grain boundaries for alloys that are susceptible to stress corrosion, subgrain boundaries for unrecrystallized alloys, or crystallographic "cleavage" planes of the {100} type. The proportion of each mode depends on ΔK, environment activity, loading frequency, alloy microstructure and specimen orientation. As an example in Figure 12, environmental fatigue in alloy 2090 occurred along subgrain boundaries at high ΔK, but by {100} "cleavage" at low ΔK when the cyclic plastic zone was contained within a single subgrain[42]. Stress intensity had no effect on the {111} slip band crack path for vacuum, helium or oxygen.

Environmental Fatigue Data Base

Most aluminum alloys are adversely affected by water vapor bearing gases and chloride containing liquids, as demonstrated by the compilation of da/dN-ΔK data in Figure 13[48,63,66-78]. For immersion in 3% NaCl at moderate ΔK and low R, corrosion fatigue may occur either above or below K_{ISCC}; da/dN is increased by 4 to 100-fold relative to helium. Crack growth in alternate immersion and salt spray environments has not been examined. Distilled water causes corrosion fatigue in aluminum alloys, Cl^- is not a requisite for cracking. Only limited data exist for near-threshold (da/dN < 10^{-6} mm/cycle) environmental fatigue crack propagation in aluminum alloys[48,66,68,79]. As illustrated in Figure 13, water vapor, moist air and aqueous chloride at free corrosion are embrittling relative to helium. Data suggest that cathodic polarization mitigates near-threshold corrosion fatigue in NaCl[42,66].

Wei and his students[69,74], Dicus[77], and Bradshaw and Wheeler[78] conducted extensive studies of the deleterious effect of pure water vapor on fatigue in 7000 and 2000 series alloys at moderate ΔK levels. Da/dN values range between an upper bound somewhat above rates for moist air and a lower bound equal to rates for inert gas. Specific data are presented in Figure 14.

Environment-Crack Closure Interactions

Crack closure must be considered when interpreting and applying environmental fatigue data, particularly for low R, near-threshold ΔK levels or rough crack surfaces. Several closure mechanisms are unique to corrosion fatigue, including wedging by corrosion debris or dislodged grains, enhanced surface roughness due to intergranular cracking, fluid pressure and environment enhanced crack wake plasticity[57]. Conversely, environment may reduce closure, for example by causing planar transgranular cleavage cracking, as reported for alloy 2090 in NaCl[75]. Owing to the difficulty of measuring crack closure loads for specimens in gaseous or aqueous environments, studies on aluminum alloys have been limited to air formed oxide induced closure; an effect that is of secondary importance[80].

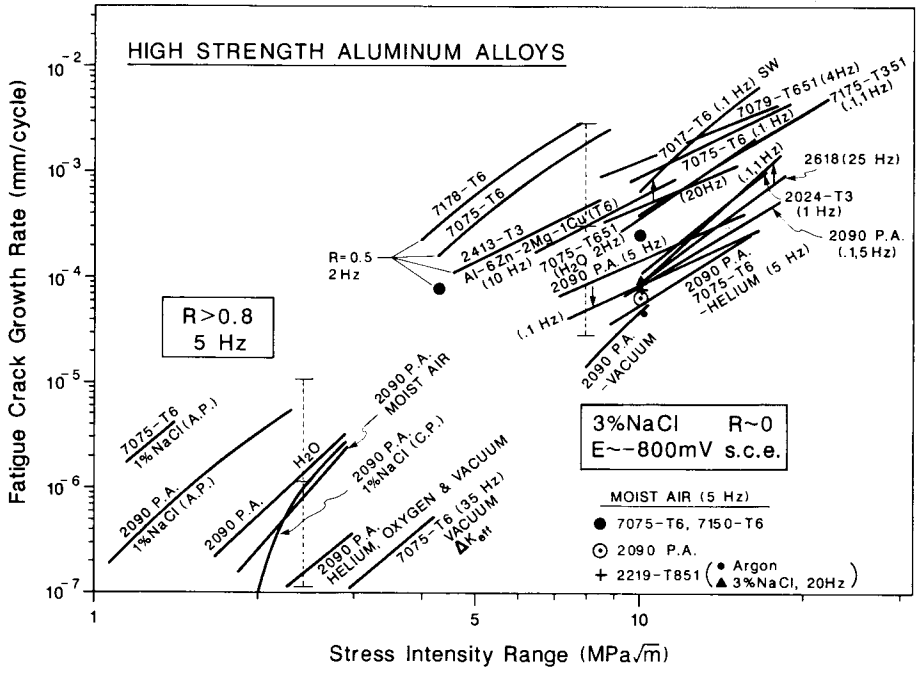

Figure 13. *Environmental fatigue crack growth data for high strength 2XXX and 7XXX series aluminum alloys.*

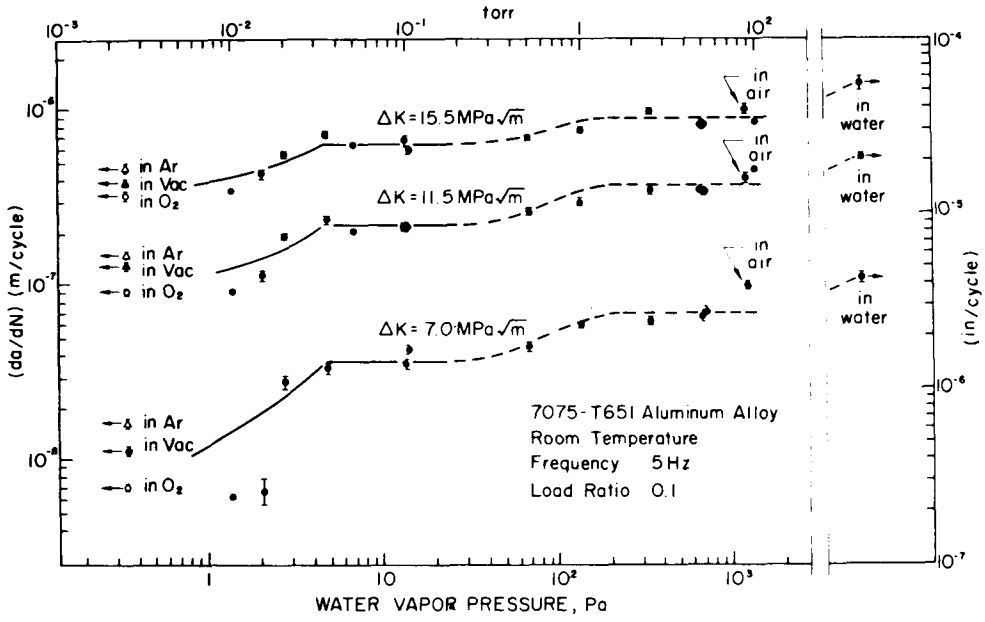

Figure 14. *Effect of water vapor pressure on crack growth rates in 7075 aluminum alloy at constant frequency and several ΔK levels (After Gao, Pao and Wei[69]).*

Important Variables

The variables listed in Table 1 affect rates of corrosion fatigue crack propagation in aluminum alloys, with complex interactions being the rule[46]. Here, it is only possible to indicate typical examples. Environment greatly complicates the dependence of da/dN on ΔK. The simple power law typical of inert environments, with a ΔK exponent between 2 and 4 and threshold behavior, is replaced by complex da/dN-ΔK relations typified by multiple regimes of power law behavior with exponents which vary from 1 to 50. Typical examples of the difference in inert and environmental da/dN-ΔK relationships are indicated in Figures 12 and 15[42,70]. Apart from decreasing closure with increasing stress ratio, the effect of R on intrinsic environmental fatigue is poorly understood.

TABLE 1 MECHANICAL, ENVIRONMENT CHEMISTRY AND METALLURGICAL VARIABLES AFFECTING ENVIRONMENTAL FATIGUE IN Al ALLOYS

STRESS INTENSITY RANGE	MEAN STRESS
CRACK SIZE AND SHAPE	SPECIMEN THICKNESS
LOADING FREQUENCY	SPECIMEN ORIENTATION
LOADING SEQUENCE	LOADING WAVEFORM
SOLUTION Cl^-, H^+, O_2, S^{-2}	WATER VAPOR PRESSURE
ELECTRODE POTENTIAL	WATER VAPOR O_2
ALLOY MICROSTRUCTURE	ALLOY COMPOSITION
GRAIN/SUBGRAIN SIZE	ALLOY YIELD STRENGTH
SLIP MORPHOLOGY	
PRECIPITATES	
TEXTURE	

Aluminum alloy composition and microstructure affect rates of environmental fatigue. Data in Figure 13 demonstrate that 7000 alloys containing Zn, Mg and Cu are more susceptible to cracking than 2000 series alloys (Al-Cu-Mg) including the new Al-Li-Cu compositions. This sensitivity parallels the well known susceptibility of 7000 alloys to intergranular SCC and hydrogen embrittlement[61,62]. Lin and Starke argue that those compositions and precipitate morphologies which promote localized intense planar slip deformation are particularly sensitive to environmental fatigue[81]. Microstructures and crack orientations which are sensitive to SCC, for example rolled plate with high angle grain surfaces parallel to the crack plane, are similarly sensitive to environmental fatigue. Wei and coworkers implicate magnesium, segregated to grain boundaries, as promoting environmental fatigue[69,82].

Environment activity (eg. water vapor pressure or electrode potential for aqueous solutions) affects crack growth rates. For NaCl, da/dN values increase with increasing anodic polarization or with strong cathodic polarization, and decrease with mild cathodic polarization[66,83]. Growth rate increases with increasing water vapor pressure to a plateau level as indicated in Figure 14[69]. Sub-part-per-million levels of water vapor cause environmental fatigue, particularly at low frequency and high stress ratio[42].

Loading frequency is perhaps the most important variable which affects environmental fatigue. Crack growth rates generally increase with decreasing frequency because increased time per loading cycle enables increased mass transport and surface reactions which favor chemically-based damage[4]. Environmental effects are often eliminated at sufficiently high loading rates; perhaps above 50 Hz, but depending on transport and reaction kinetics. Frequency effects are predicted for environmental fatigue above K_{ISCC}, a purely time-dependent phenomena. Here, the environmental contribution to inert environment da/dN increases linearly with the amount of time per load cycle while the cyclic stress intensity is above the threshold for SCC[67,84]. Crack growth below K_{ISCC} is both cycle and time-dependent, and is a more complex case to predict.

A typical example of the time dependence of environmental fatigue below K_{ISCC} is given in Figure 15 for

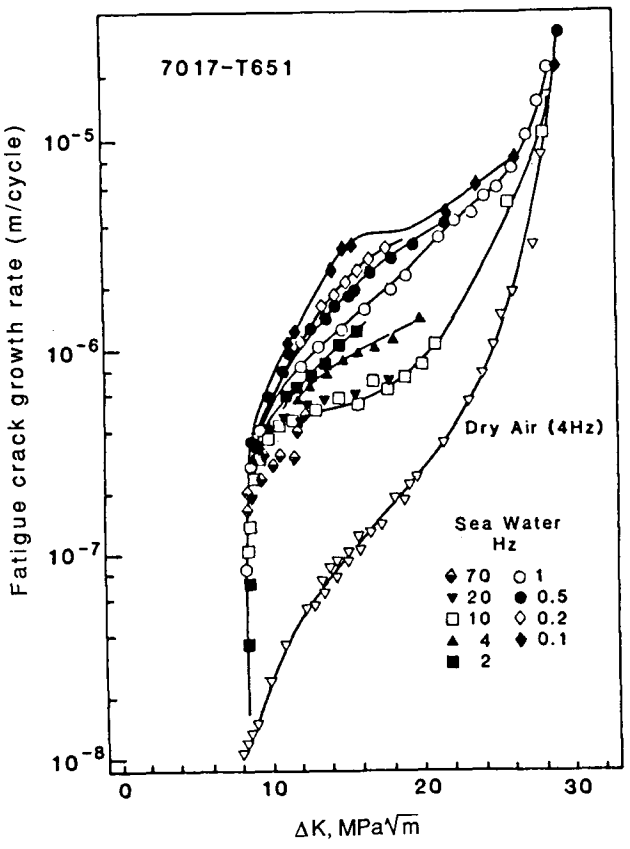

Figure 15. *Effects of environment and loading frequency on crack growth rates in alloy 7017 (After Holroyd and Hardie[70]).*

alloy 7017 in aqueous chloride[70]. While cracking in inert dry air is independent of frequency, environmental fatigue is enhanced by decreasing frequency from 70 to 0.1 Hz. Similar data were reported for water vapor; the results in Figure 14 are well represented by the ratio of water vapor pressure to loading frequency[69,74,77,78]. In rare instances da/dN increases mildly with increasing frequency[42].

Interactions of variables often complicate the trends cited here. For example, the frequency effect indicated in Figure 15 varies with ΔK and probably electrode potential. Strong frequency effects at higher ΔK may be replaced by frequency insensitivity near threshold[46].

Environmental Fatigue Mechanisms

One of three mechanisms is typically cited to explain environmental effects on fatigue in aluminum alloys; hydrogen environment embrittlement, film rupture/electrochemical repassivation, and crack surface film effects on dislocations[46,65,85,86]. These processes are speculative and the topic of intense research.

Based on circumstantial evidence, hydrogen embrittlement is cited as a damage mechanism for environmental fatigue of aluminum alloys in water vapor[4,42,68,69,74,79,87,88] and chloride electrolytes[42,61,67,70,85]. In this view atomic hydrogen chemically adsorbs on clean crack tip surfaces as the result of either gas molecule-surface chemical reactions or electrochemical cathodic reduction of hydrogen ions or water molecules coupled with local anodic dissolution. Hydrogen production follows mass transport within the crack environment and precedes hydrogen atom diffusion in the crack tip plastic zone to sites of fatigue damage. Environmental crack growth rates are limited by one or more slow steps in this transport/reaction sequence[4,69,70,89]. The atomistic processes for hydrogen embrittlement are unknown.

Models of environmental fatigue were developed based on a repeating sequence of film rupture and anodic repassivation[90-92]. In this view localized plastic straining ruptures an otherwise protective film at the crack tip. Crack advance occurs during transient anodic dissolution of the metal at the film breach and while the surface repassivates. Quantitative models for da/dN include metal dissolution and repassivation kinetics, film ductility and crack tip strain rate. This model has been extensively applied to steels in aqueous environments[90,92], however, applications to aluminum alloys are limited[93].

Given important assumptions and adjustable parameters, hydrogen and film rupture models quantitatively predict da/dN-ΔK, as necessary to extrapolate data over a broad range of variables[46]. These expressions emphasize the mass transport and chemical reaction components of fatigue damage and are capable of predicting environment chemistry, metallurgical and time variables. A typical result is the predicted exposure (water vapor pressure to frequency ratio) dependence of da/dN indicated by the solid lines in Figure 14[69,74]. These models are, however, limited because it is not possible to directly probe crack tip process zone damage on the microscopic scale; the specific fatigue damage mechanism has not been defined.

Life Prediction Methods

Life prediction codes do not adequately deal with environmental effects on fatigue crack propagation. Recent successes have been reported for steels in offshore oil and gas structures, and in piping and pressure vessel components of nuclear power systems[5,9].

Several aspects of environmental fatigue complicate fracture mechanics life prediction. The strong effect of loading frequency hinders the application of laboratory data, obtained over short time periods on the order of days, to describe the long life (viz. years) performance of a component in an aggressive environment. Predictions are further complicated by the many variables which affect crack growth rate behavior. Lacking mechanistically based models, da/dN-ΔK data must be obtained for the specific time, mechanical, chemical and metallurgical conditions of interest.

VII. Variable Amplitude Loading

An improved understanding of the crack growth process under constant amplitude loading is essential in the development of crack growth life prediction methods under variable amplitude loading. For spectrum loading, crack growth rates tend to span many orders of magnitude and, consequently, an accurate description of constant amplitude data over many orders of magnitude in rates is necessary to predict accurate lives. Constant amplitude data provide information on microstructural effects, ΔK_{th}, short crack effects, transitions in the ΔK-rate curve[94], flat-to-slant crack growth, constraint (specimen thickness) effects, nonplanar crack profiles (shear lip, mixed-mode behavior), crack closure, stress level and stress ratio effects. To develop improved life prediction methods, crack closure mechanisms must be understood and analysis methods must be developed to calculate the variation in closure as a function of load history, thickness, environment and material.

A review of the current understanding of crack growth processes and the status of prediction methodologies under variable-amplitude loading is given by Wanhill and Schijve[95]. They identified an important observation from crack growth rate tests conducted under flight simulation loading. Flight simulation tests that are conducted on thin specimens of ductile alloys show an initial decrease in crack growth rate per flight, whereas thicker specimens show an immediate rise in rates, as shown in Figure 16. The solid curves show test results on 2 and 10 mm thick center crack tension specimens made of 2024-T351 aluminum alloy[96]. Both specimens had a 4 mm sharp notch (c_n = 4 mm) at the center of the specimen to initiate the cracks and were subjected to the Mini-TWIST[97] load spectrum (clipped at level III) with a mean stress, S_{mf} of 70 MPa. The dashed curves show the predicted crack growth rates from the analytical crack closure model[17] using the variable constraint option[21,60] to correlate the constant amplitude data. The predicted rates agree well with the measured rates, especially for the thick material. Some differences were observed between the experiment and analyses in the early stages of growth in the thick specimen. This discrepancy may be due to faster crack growth in the interior of the specimen than at the surface. The early stage of growth in the thin specimen was predicted quite well by the closure model. The ratio of predicted-to-test lives (from c = 4 mm to failure) were 0.68 and 1.06 for the thin and thick specimens, respectively. Blom[98] has shown similar results under the TWIST spectrum, using the variable constraint method that was developed in the FASTRAN code. Future damage tolerant codes should incorporate advanced closure models (eg. Reference 17) to improve predictive capabilities.

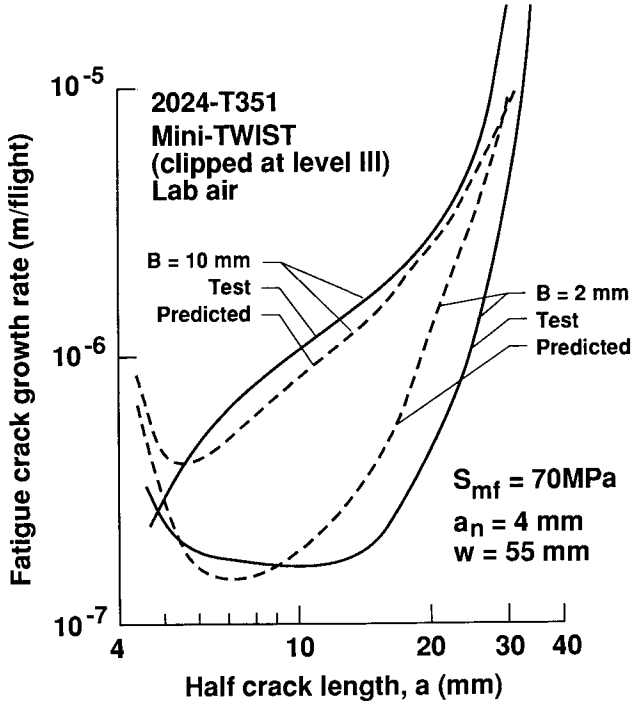

Figure 16. *Comparisons of experimental and predicted mean crack growth rates under Mini-TWIST spectrum loading.*

VIII. Future Directions

While the fracture mechanics approach provides an effective means to characterize and to predict fatigue crack propagation in aerospace aluminum alloy components, significant research and engineering uncertainties must be addressed.

Experiments must be conducted to determine:

(1) Environmental effects on near-threshold crack propagation, particularly as a function of loading frequency, and identifying the contributions of extrinsic closure and intrinsic fatigue damage.

(2) Fatigue crack propagation behavior of advanced light alloys and composites. Environmental effects, crack closure, spectrum loading effects and the extent to which fatigue damage is distributed or heterogeneous and not described by continuum fracture mechanics must be defined.

(3) Environmental fatigue crack propagation under complex spectrum loading, including the effects of single and multiple over/under-loads and load history.

(4) Crack closure phenomena for aggressive environments.

(5) Fractographic descriptions of the micromechanisms of fatigue crack propagation as a function of the controlling variables, particularly environment.

(6) Accelerated measurement of near-threshold da/dN and for *in situ* monitoring of defect-based initiation, early crack growth kinetics and closure evolution for microstructurally small fatigue cracks in inert and aggressive environments.

(7) Measurement of fatigue crack chemistry, surface reaction kinetics and crack tip process zone microscopic damage.

Modeling must be conducted to address:

(1) Crack closure in aggressive environments and under complex loading histories. Models must be developed for roughness and corrosion product mechanisms.

(2) Hydrogen production or film formation/rupture, integrated with microscopic process zone fatigue damage to predict environmental da/dN-ΔK.

(3) Life prediction codes which incorporate environmental effects on crack growth, extrapolated from short term laboratory data.

(4) Life prediction codes which incorporate short crack effects, crack closure and spectrum loading.

(5) Comparisons of code predictions with damage sensor data and large scale component experiments.

References

1. P.C. Paris, M.P. Gomez and W.E. Anderson, The Trend in Engineering, Washington State Univ., Vol. 13, No. 1, pp. 9-14 (1961).
2. R. W. Hertzberg, Deformation and Fracture Mechanics of Engineering Materials, Ch. 13, 2nd Ed., John Wiley and Sons, New York (1983).
3. "Standard Test Method for Measurement of Fatigue Crack Growth Rates", ASTM Standard E647-88, ASTM Book of Standards, Vol. 03.01, pp. 899-926, ASTM, Philadelphia, PA (1988).
4. R.P. Wei and R.P. Gangloff, in Fracture Mechanics: Perspectives and Directions, ASTM STP 1020, R.P. Wei and R.P. Gangloff, eds., ASTM, Philadelphia, Pa, pp. 233-264 (1989).
5. P.L. Andresen, R.P. Gangloff, L.F. Coffin and F.P. Ford, in Fatigue 87, R.O. Ritchie and E.A. Starke, Jr., eds., EMAS, West Midlands, England, pp. 1723-1751 (1987).
6. B. Tompkins and P.M. Scott, Metals Tech., Vol. 9., pp. 240-248 (1982).
7. J.M. Barsom and S.R. Novak, "Subcritical Crack Growth and Fracture of Bridge Steels", National Cooperative Highway Research Report 181, National Research Council, Washington, DC (1977).
8. O. Vosikovsky and R.J. Cooke, Int. J. Pres. Ves. & Piping, Vol. 6, pp. 113-129 (1978).
9. S.J. Hudak, O.H. Burnside and K.S. Chan, J. Energy Resources Tech., ASME Trans., Vol. 107, pp. 212-219 (1985).
10. J.B. Chang and C.M. Hudson, eds., Methods and Models for Predicting Fatigue Crack Growth Under Random Loading, ASTM STP 748, ASTM, Philadelphia, PA (1981).
11. H.H. van der Linden, "A Check of Crack Propagation Prediction Models Against Test Results Generated Under Transport Aircraft Flight Simulation Loading", NLR TR 84005 U (GARTEUR/TP-008), National Aerospace Laboratory, The Netherlands, December (1983).
12. J.D. Willenborg, R.M. Engle and H.A. Wood, "A Crack Growth Retardation Model Using an Effective Stress Concept", AFFDL-TM-71-1-FBR, Air Force Flight Dynamics Laboratory (1971).
13. J.P. Gallagher, "A Generalized Development of Yield Zone Models", AFFDL-TM-74-28-FBR, Air Force Dynamics Laboratory, January (1974).
14. W.S. Johnson, in Methods and Models for Predicting Fatigue Crack Growth Under Random Loading, ASTM STP 748, J.B. Chang and C.M. Hudson, eds., ASTM, Philadelphia, PA, pp. 85-102 (1981).
15. A.U. de Koning and H.H. van der Linden, "Prediction of Fatigue Crack Growth Rates Under Variable Loading Using a Simple Crack Closure Model", NLR MP 81023 U, April (1981).
16. G. Baudin and M. Robert, "Crack Growth Model for Flight-Type Loading", Proceedings of 11th ICAF Symposium, Noordwijkerhout, The Netherlands, May (1981).
17. J.C. Newman, Jr., in Methods and Models for Predicting Fatigue Crack Growth Under Random Loading, ASTM STP 748, J.B. Chang and C.M. Hudson, eds., ASTM, Philadelphia, PA, pp. 53-84 (1981).
18. J.B. Chang, M. Szamossi and K.W. Liu, "User's Manual for a Detailed Level Fatigue Crack Growth Analysis Computer Code - CRKGRO", AFWAL-TR-3093, November (1981).
19. R.G. Forman, V. Shivakumar, J.C. Newman, Jr., S.M. Piotrowski and L.C. Williams, in Fracture Mechanics: Eighteenth Symposium, ASTM STP 945, ASTM, Philadelphia, PA, pp. 781-803 (1988).
20. NASCRAC--NASA Crack Analysis Code User's Manual, Failure Analysis Associates, Inc., Palo Alto, CA (1989).
21. FASTRAN--Fatigue Crack Growth Analysis--A Closure Model, Computer Software Management and Information Center, University of Georgia, Athens, Georgia, December (1984).
22. J.C. Newman, Jr. and W. Elber, eds., Mechanics of Fatigue Crack Closure, ASTM STP 982, ASTM, Philadelphia, PA (1988).
23. W. Elber, in Damage Tolerance in Aircraft Structures, ASTM STP 486, pp. 230-247 (1971).
24. G.T. Gray, J.C. Williams and A.W. Thompson, Metall. Trans. A, Vol. 14A, pp. 421-433 (1983).

25. S. Suresh, G.F. Zaminski and R.O. Ritchie, Metall. Trans. A, Vol. 12A, pp. 1435-1443 (1981).

26. S. Suresh and R.O. Ritchie, in Fatigue Crack Growth Threshold Concepts, AIME, Warrendale, PA, pp. 227-261 (1984).

27. R.O. Ritchie, Mat. Sci. Eng., Vol. 103, pp. 15-28 (1988).

28. H.L. Ewalds, Eng. Frac. Mech., Vol. 13, pp. 1001-1007 (1980).

29. C.M. Hudson, "Effect of Stress Ratio on Fatigue Crack Growth in 7075-T6 and 2024-T3 Aluminum Alloy Specimens", NASA TN D-5390 (1969).

30. R.G. Dubensky, "Fatigue Crack Propagation in 2024-T3 and 7075-T6 Aluminum Alloys at High Stresses", NASA CR-1732 (1971).

31. E.P. Phillips, in Mechanics of Fatigue Crack Growth, ASTM STP 982, J.C. Newman, Jr. and W. Elber, eds., ASTM, Philadelphia, PA, pp. 505-515 (1988).

32. J.C. Newman, Jr., C.C. Poe, Jr. and D.S. Dawicke, "Proof Test and Fatigue Crack Growth Modeling on 2024-T3 Aluminum Alloy", to be presented at International Conference on Fatigue, Honolulu, Hawaii (1990).

33. M.O. Speidel, in Stress Corrosion Cracking and Hydrogen Embrittlement of Iron Based Alloys, J. Hochmann, J. Slater, R.D. McCright and R.W. Staehle, eds., NACE, Houston, TX, pp. 1071-1094 (1977).

34. W.A. Herman, R.W. Hertzberg and R. Jaccard, J. Fat. and Frac. of Engr. Matls. and Struc., Vol. 11, pp 303-320 (1988).

35. D.L. Davidson and S. Suresh, eds. Fatigue Crack Growth Threshold Concepts, TMS-AIME, Warrendale, PA (1984).

36. D. Taylor, A Compendium of Fatigue Thresholds and Growth Rates, Engineering Materials Advisory Services, Ltd., West Midlands, UK (1985).

37. R.O. Ritchie and W. Yu, in Small Fatigue Cracks, R.O. Ritchie and J. Lankford, eds., TMS-AIME, Warrendale, PA, pp. 167-189 (1986).

38. J.K. Donald, "Closure Measurement Techniques", Presented at the ASTM E24.04 Research Task Group Meeting, Atlanta, GA (1988).

39. E. Zaiken and R.O. Ritchie, Engr. Fract. Mech., Vol. 22, No. 1, pp. 35-46 (1985).

40. M.R. James, Scripta Met., Vol. 21, pp. 783-788 (1987).

41. J.K. Donald, unpublished research, Fracture Technology Associates, Springtown, PA (1989).

42. R.S. Piascik, "Intrinsic Damage Localization During Corrosion Fatigue: Al-Li-Cu System", PhD Dissertation, University of Virginia (1990).

43. A.K. Vasudevan and P.E. Bretz, in Fatigue Crack Growth Threshold Concepts, D.L. Davidson and S. Suresh, eds.,TMS-AIME, Warrendale, PA, pp. 25-42 (1984).

44. E.A. Starke, Jr. and G. Lutering, in Fatigue and Microstructure, ASTM, Metals Park, OH, pp. 205-243 (1979).

45. K.T. Venkateswara Rao, R.S. Piascik, R.P. Gangloff and R.O. Ritchie, in Proc. Fifth Intl. Al-Li Conf., T.H. Sanders, Jr. and E.A. Starke, Jr., eds., Materials and Component Engineering Publications Ltd., Birmingham, UK, pp. 955-971 (1989).

46. R.P. Gangloff, in Environment Induced Cracking in Metals, R.P. Gangloff and M.B. Ives, eds., NACE, Houston, TX, pp. 55-109 (1990).

47. K.T. Venkateswara Rao and R.O. Ritchie, "Fatigue-Crack Propagation in Advanced Aerospace Materials: Aluminum-Lithium Alloys", to be published in Advances in Fracture Research, K. Salama, K. Ravi-Chandar, D.M.R. Taplin and P. Rama Rao, eds., Pergamon Press, London (1989).

48. R.S. Piascik and R.P. Gangloff, in Advances in Fracture Research, K. Salama, K. Ravi-Chandar, D.M.R. Taplin and P. Rama Rao, eds., Pergamon Press, London, pp. 907-918 (1989).

49. A.J. McEvily, "The Fatigue of Powder Metallurgy Alloys", Annual Report, U.S. Air Force Grant No. AFOSR 81-0046, University of Connecticut, Storrs, CT (1982).

50. C.P. Blankenship, Jr. and E.A. Starke, Jr., "The Fatigue Crack Growth Behavior of the Al-Cu-Li Alloy 049", unpublished research, University of Virginia, Charlottesville, VA (1990).

51. G.H Bray, unpublished research, University of Virginia, Charlottesville, VA (1990).

52. J.C. Newman, Jr. and P.R. Edwards, eds., "Short-Crack Growth Behavior in an Aluminum Alloy - An AGARD Cooperative Test Program", AGARD Report No. 732 (1988).

53. P.R. Edwards and J.C. Newman, Jr., eds., "Short-Crack Growth Behavior in Various Aircraft Materials", AGARD Report No. 767 (1990).

54. R.O. Ritchie and J. Lankford, eds., Small Fatigue Cracks, TMS-AIME, Warrendale, PA (1986).

55. R.O. Ritchie and J. Lankford, Matls. Sci. Engr., Vol. 84, pp. 11-16 (1986).

56. S. Suresh and R.O. Ritchie, Int. Metall. Rev., Vol. 29, pp. 445-476 (1984).

57. R.P. Gangloff and R.O. Ritchie, in Fundamentals of Deformation and Fracture, B.A. Bilby, K.J. Miller and J.R. Willis, eds., Cambridge University Press, Cambridge, UK, pp. 529-558 (1985).

58. R.P. Gangloff and R.P. Wei, in Small Fatigue Cracks, R.O. Ritchie and J. Lankford, eds., TMS-AIME, Warrendale, PA, pp. 239-264 (1986).

59. S.J. Hudak, J. Engr. Matls. Tech., Vol. 103, pp. 26-35 (1981).

60. J.C. Newman, Jr., M.H. Swain, and E.P. Phillips, in Small Fatigue Cracks, R.O. Ritchie and J. Lankford, eds., TMS-AIME, Warrendale, PA, pp. 427-452 (1986).

61. M.O. Speidel, Metall. Trans. A, Vol. 6A, pp. 631-651 (1975).

62. N.J.H. Holroyd and G.M. Scamans, in Environment Induced Cracking of Metals, R.P. Gangloff and M.B. Ives, eds., NACE, Houston, TX, pp. 311-346 (1990).

63. J.A. Feeney, J.C. McMillan and R.P. Wei, Met. Trans., Vol. 1, pp. 1741-1757 (1970).

64. R.P. Gangloff, et al., in Metals Handbook: Mechanical Testing, Vol. 8, 9th Ed., ASM International, Metals Park, OH, pp. 403-435 (1985).

65. D.J. Duquette, in Environment Induced Cracking of Metals, R.P. Gangloff and M.B. Ives, eds., NACE, Houston, TX, pp. 45-54 (1990).

66. R.S. Piascik and R.P. Gangloff, in Environment Induced Cracking of Metals, R.P. Gangloff and M.B. Ives, eds., NACE, Houston, TX, pp. 233-240 (1990).

67. M.O. Speidel, M.J. Blackburn, T.R. Beck and J.A. Feeney, in Corrosion Fatigue, Chemistry, Mechanics and Microstructure, O. Devereux, A.J. McEvily and R.W. Staehle, eds., NACE, Houston, TX, pp. 324-345 (1972).

68. J. Petit and A. Zeghloul, "Environmental Influence on Threshold and Near Threshold Behavior of Short and Long Fatigue Cracks", Environment Assisted Cracking: Science and Engineering, ASTM STP 1049, T.W. Crooker and W.B. Lisagor, eds., ASTM, Philadelphia, PA, in press (1990).

69. M. Gao, P.S. Pao and R.P. Wei, Metall. Trans. A, Vol. 19A, pp. 1739-1750 (1988).

70. N.J.H. Holroyd and D. Hardie, Corrosion Science, Vol. 23, pp. 527-546 (1983).

71. K. Jata and E.A. Starke, Jr., Metall. Trans. A., Vol. 17A, pp. 1011-1026 (1986).

72. D. Aliaga and E. Budillon, "Corrosion Fatigue Behavior of Some Aluminum Alloys", AGARD Report No. AGARD-CP-316 (1981).

73. R.J. Selines and R.M. Pelloux, Met. Trans., Vol. 3, pp. 2525-2531 (1972).

74. R.P. Wei, P.S. Pao, R.G. Hart, T.W. Weir and G.W. Simmons, Metall. Trans. A, Vol. 11A, pp. 151-158 (1980).

75. P.S. Pao, M.A. Imam, L.A. Cooley and G.R. Yoder, Corrosion, Vol. 45, pp. 530-535 (1989).

76. N. Ranganathan, M. Quintard and J. Petit, "Environmental Influence on the Effect of a Single Overload on the Fatigue Crack Growth Behavior of a High Strength Aluminum Alloy", in Environment Assisted Cracking: Science and Engineering, ASTM STP 1049, T.W. Crooker and W.B. Lisagor, eds., ASTM, Philadelphia, PA, in press (1990).

77. D.L. Dicus, in Environment Sensitive Fracture: Evaluation and Comparison of Test Methods, ASTM STP 821, S.W. Dean, E.N. Pugh and G.M. Ugiansky, eds., ASTM, Philadelphia, PA, pp. 513-533 (1984).

78. F.J. Bradshaw and C. Wheeler, Intl. J. Frac. Mech., Vol. 5, pp. 255-268 (1969).

79. A. Niegel, H.-J. Gudladt and V. Gerold, in Fatigue 87, R.O. Ritchie and E.A. Starke, Jr., eds., EMAS, West Midlands, UK, pp. 1229-1238 (1987).

80. S. Suresh, A.K. Vasudevan and P.E. Bretz, Metall. Trans. A., Vol. 15A, pp. 369-379 (1984).

81. F.S. Lin and E.A. Starke, Jr., in Hydrogen Effects in Metals, I.M. Bernstein and A.W. Thompson, eds., TMS-AIME, Warrendale, PA, pp. 485-492 (1981).

82. N.J.H. Holroyd and G.M. Scamans, Scripta Metall., Vol. 19, pp. 915-916 (1985).

83. R.E. Stoltz and R.M. Pelloux, Met. Trans., Vol. 3, pp. 2433-2441 (1972).

84. M.O. Speidel, Unpublished research (1975), reported in J.C. Scully, in Environment Sensitive Fracture of Engineering Materials, Z.A. Foroulis, ed., TMS-AIME, Warrendale, PA, pp. 71-90 (1979).

85. D.J. Duquette, "Mechanisms of Corrosion Fatigue of Aluminum Alloys", AGARD Report No. AGARD-CP-316 (1981).

86. N.M. Grinberg, Intl. J. Fatigue, April, pp. 83-95 (1982).

87. W. Gruhl, Z. Metallkde, Vol. 75, pp. 819-826 (1984).

88. R.E. Ricker and D.J. Duquette, Metall. Trans. A, Vol. 19A, pp. 1775-1783 (1988).

89. R.P. Wei, "Corrosion Fatigue Crack Growth and Reactions with Bare Steel Surfaces", Corrosion 89, Paper No. 569, NACE, Houston, TX (1989).

90. F.P. Ford, J. Press. Ves. Tech., Trans. ASME, Vol. 110, pp. 113-128 (1988).

91. P.L Andresen and F.P. Ford, Matls. Sci. Engr., Vol. A103, pp. 167-184 (1988).

92. S.J. Hudak, "Corrosion Fatigue Crack Growth: The Role of Crack-Tip Deformation and Film Formation Kinetics", PhD Dissertation, Lehigh University, Bethlehem, PA (1988).

93. F.P. Ford, Corrosion, Vol. 35, pp. 281-287 (1979).

94. G.R. Yoder, L.A. Cooley and T.W. Crooker, "On Microstructural Control of Near-Threshold Fatigue Crack Growth in 7000-Series Aluminum Alloys", NRL Memorandum Report 4787, Naval Research Laboratory, Washington, April (1982).

95. R.J.H. Wanhill and J. Schijve, "Current Status of Flight Simulation Fatigue Crack Growth Concepts", NLR MP 88001 U (1988).

96. R.J.H. Wanhill, private communication (1990).

97. H. Lowak, J.B. de Jonge, J. Franz and D. Schutz, "Mini-TWIST, a Shortened Version of TWIST", National Aerospace Laboratory, NLR MP-79018 (1979). (Also, LBF-Report TB-146.)

98. A.F. Blom, "Spectrum Fatigue Crack Growth: Numerical Modelling", presented the International Conference on Fatigue Crack Growth under Variable Amplitude Loading, Paris, France, June (1988).